

# Dietary Energy Restriction Modulates the Activity of AMP-Activated Protein Kinase, Akt, and Mammalian Target of Rapamycin in Mammary Carcinomas, Mammary Gland, and Liver

Wei Qin Jiang, Zongjian Zhu, and Henry J. Thompson

Cancer Prevention Laboratory, Colorado State University, Fort Collins, Colorado

## Abstract

**Dietary energy restriction (DER) inhibits mammary carcinogenesis, yet mechanisms accounting for its protective activity have not been fully elucidated. In this study, we tested the hypothesis that DER exerts effects on intracellular energy sensing pathways, resulting in alterations of phosphorylated proteins that play a key role in the regulation of cancer. Experiments were conducted using the 1-methyl-1-nitrosourea-induced mammary cancer model in which rats were 0%, 20%, or 40% energy restricted during the postinitiation stage of carcinogenesis. Parallel experiments were done in non-carcinogen-treated rats in which effects of DER at 0%, 5%, 10%, 20%, or 40% in liver were investigated. In a DER dose-dependent manner, levels of Thr<sup>172</sup> phosphorylated AMP-activated protein kinase (AMPK) increased in mammary carcinomas with a concomitant increase in phosphorylated acetyl-CoA-carboxylase, a direct target of AMPK, the phosphorylation of which is regarded as an indicator of AMPK activity. Levels of phosphorylated mammalian target of rapamycin (mTOR) decreased with increasing DER, and down-regulation of mTOR activity was verified by a decrease in the phosphorylation state of two mTOR targets, 70-kDa ribosomal protein S6 kinase (p70S6K) and eukaryote initiation factor 4E binding protein 1 (4E-BP1). Coincident with changes in mTOR phosphorylation, levels of activated protein kinase B (Akt) were also reduced. Similar patterns were observed in mammary glands and livers of non-carcinogen-treated rats. This work identifies components of intracellular energy sensing pathways, specifically mTOR, its principal upstream regulators, AMPK and Akt, and its downstream targets, p70S6K and 4E-BP1, as candidate molecules on which to center mechanistic studies of DER.** [Cancer Res 2008;68(13):5492-9]

## Introduction

Dietary energy restriction (DER) reduces carcinogenesis at multiple organ sites including breast and liver (1-5). This well-established phenomenon occurs in a dose-dependent manner and is remarkably reproducible across animal models. Much of the effort in this field to elucidate the mechanisms that account for DER inhibitory activity has focused either on the identification of the cellular processes affected (i.e., proliferation, apoptosis, and

angiogenesis) or on the systemic factors that may mediate protective activity, primarily insulin-like growth factor I (IGF-I), adrenal cortical steroids, and adipokines such as leptin (6-10). Inhibition of carcinogenesis by DER involves decreased cell proliferation, increased sensitivity to cell death via apoptosis, and decreased density in the amount of blood vessels supplying a tumor (4). For a number of years, it was judged that the key to elucidating the powerful effects of DER on these cellular processes might lie in the understanding of the alterations of systemic factors like glucocorticoids and IGF-I, and certainly, those studies have given the field important insights (3, 4). However, experiments designed to determine whether DER-mediated changes in plasma concentrations of glucocorticoids or IGF-I are obligatory for protection against mammary cancer indicated that knowledge of effects on these systemic factors was not sufficient to identify all the mechanisms that account for DER-mediated protection (7, 10).

Despite well-recognized changes in energy metabolism known to occur during the development of cancer (11, 12), little attention has been given to the possibility that a key to identifying the critical pathways involved in DER-mediated inhibition of carcinogenesis lies within the cell and is triggered, in part, by the effects of DER on intracellular energy sensing mechanisms. We hypothesized that DER would activate an ancient intracellular fuel sensor, AMP-activated protein kinase (AMPK), and, in concert with DER effects on IGF-I signaling that are mediated via protein kinase B (Akt), would work to down-regulate the activity of the mammalian target of rapamycin (mTOR). Measurement of AMPK activation served as a primary end point for this work because a growing body of evidence indicates that AMPK functions as a fuel sensor in many tissues and organs where it inhibits anabolic pathways when cellular ATP levels are reduced and when AMP increases in response to limited energy availability (13). Moreover, because activation of AMPK by phosphorylation has been reported to inhibit the activity of mTOR, the phosphorylation-mediated activation of 70-kDa ribosomal protein S6 kinase (p70S6K), and the phosphorylation-dependent inactivation of eukaryote initiation factor 4E binding protein 1 (4E-BP1; refs. 14-16), events linked to the inhibition of cell proliferation and angiogenesis and induction of a proapoptotic environment, we hypothesized that mTOR activity would be down-regulated by DER; these molecules served as additional end points in our analyses. Because down-regulation of the signaling pathway, whose components are IGF-I receptor (IGF-IR), phosphatidylinositol 3-kinase (PI3K), and Akt, has been shown to be associated with DER, and this pathway is linked to the regulation of mTOR (17-20), these molecules were also measured. The linkage of signaling through the IGF-IR pathway to mTOR is specifically attributed to one of its activated mediators, phosphorylated Akt, which has been reported to oppose the effects of phosphorylated AMPK on the activity of mTOR and its downstream targets (21), thus providing an additional rationale for the

**Note:** Supplementary data for this article are available at Cancer Research Online (<http://cancerres.aacrjournals.org/>).

**Requests for reprints:** Henry J. Thompson, Cancer Prevention Laboratory, Colorado State University, 1173 Campus Delivery, Fort Collins, CO 80523. Phone: 970-491-7748; Fax: 970-491-3542; E-mail: henry.thompson@colostate.edu.

©2008 American Association for Cancer Research.  
doi:10.1158/0008-5472.CAN-07-6721

pathways investigated. Our initial analyses were done on mammary carcinomas and then selectively extended to lysates of mammary gland excised from the same rats in which no evidence of premalignant or malignant mammary pathologies was apparent (referred to as pathology-free). Having obtained evidence consistent with an effect of DER on these energy sensing mechanisms, a second experiment was done in non-carcinogen-treated rats. This was done to extend our observations to another organ site in which carcinogenesis is inhibited by DER via similar cellular mechanisms (5, 22) and to more rigorously test our hypothesis in a tissue that is relatively homogeneous in terms of cell types present. This approach permitted more detailed analyses than were possible using the limited amount of pathology-free mammary tissue available from our first experiment, and it allowed us to extend the work to less stringent levels (5% and 10%) of DER. Thus, the goal of the work reported herein was to establish whether DER affects the activity of the energy sensing network whose components are AMPK, Akt, and mTOR.

## Materials and Methods

**Chemicals.** Primary antibodies used in this study were anti-phospho-AMPK (Thr<sup>172</sup>), anti-AMPK, anti-phospho-mTOR (Ser<sup>2448</sup>), anti-mTOR, anti-phospho-p70S6K (Thr<sup>389</sup>), anti-p70S6K, anti-phospho-4E-BP1 (Thr<sup>37/46</sup>), anti-4E-BP1, anti-phospho-Akt (Ser<sup>473</sup>), anti-Akt, anti-phospho-acetyl-CoA-carboxylase (ACC; Ser<sup>79</sup>), anti-ACC, anti-PI3Kp85, anti-PI3Kp110 $\alpha$ , anti-phospho-tuberosus sclerosis complex 2 (TSC2; Thr<sup>1462</sup>), anti-TSC2, and antirabbit immunoglobulin horseradish peroxidase (HRP)-conjugated secondary antibody, as well as LumiGLO reagent with peroxide, all from Cell Signaling Technology. Anti-IGF-IR antibody and antimouse immunoglobulin HRP-conjugated secondary antibody were from Santa Cruz Biotechnology. Anti-LKB1 antibody was from Millipore. Mouse anti- $\beta$ -actin primary antibody was obtained from Sigma Chemical Co. A mTOR Kinase Activity Assay kit was purchased from (EMD). Tris-glycine gels were purchased from Invitrogen.

**Animals, housing, and diets.** Female Sprague-Dawley rats were obtained from Taconic Farms at 20 d of age and were housed individually in stainless steel metabolic cages with wire mesh bottoms from 23 d of age to the end of an experiment. The cages were equipped with adjustable width external tunnel feeders that permitted accurate quantification of food intake. All rats were fed a modified AIN-93G diet formulation as previously described (23). The animal facility in which the rats were housed is Association for Assessment and Accreditation of Laboratory Animal Care accredited. The animal room was maintained at 22  $\pm$  1°C with 50% relative humidity and a 12-h light/12-h dark cycle. The work reported was reviewed and approved by Colorado State University Animal Care and Use Committee and conducted according to the guidelines of the committee.

### Experiment 1

**Experimental design.** At 21 d of age, rats were injected with 50 mg of 1-methyl-1-nitrosourea/kg body weight (i.p.) as previously described (24). Five days following carcinogen injection, all rats were randomized into three groups ( $n$  = 30 per group) and meal fed AIN-93G control diet *ad libitum* (control), a modified AIN-93G diet in an amount that was 80% of *ad libitum* intake of the control (20% DER), or a modified AIN-93G diet in an amount that was 60% of *ad libitum* intake of the control (40% DER; ref. 23). All of the rats were meal fed twice daily (8:00–11:00 a.m. and 2:00–5:00 p.m.), 7 d a week to reduce possible confounding due to intergroup variation in meal timing, meal number, and duration of fasting between meals. Rats in the control group were allowed access to an unlimited amount of diet each meal whereas rats in DER groups were given a restricted amount that was equally divided to two meals and provided in each meal twice per day. The diet fed to 20% or 40% DER rats was formulated to ensure an intake of all nutrients equivalent to the control group while limiting total dietary energy by reducing carbohydrate. All rats were palpated thrice a week for detection

of mammary tumors beginning at 19 d post-carcinogen until study termination at 52 d post-carcinogen (73 d of age).

**Necropsy and sample collection.** Following overnight fast and inhalation of gaseous carbon dioxide and cervical dislocation, rats were then skinned and the skin area with the mammary gland chain was examined under translucent light to locate mammary tumors. The tumors were excised and snap frozen in liquid nitrogen. The contralateral abdominal inguinal mammary gland chain was excised, prepared as a whole mount on transparency film, and snap frozen in liquid nitrogen. All samples were stored at  $-80^{\circ}\text{C}$ . Only mammary adenocarcinomas and pathology-free mammary gland number 4 from the same tumor bearing rat were evaluated (7–9 rats per group).

### Experiment 2

**Experimental design.** Rats were randomized by body weight at 23 d of age and divided into each of five groups (eight rats per group). Rats in all groups were meal fed the same diet formulations as described in experiment 1, 3 h per meal, 2 meals per day, 7 d per week. Rats in the control (DER 0%) group were allowed access to an unlimited amount of diet each meal whereas rats in DER groups were given a restricted amount that was equally divided to two meals and provided in each meal twice per day. The four groups of restricted-fed rats were given 95% (DER 5%), 90% (DER 10%), 80% (DER 20%), or 60% (DER 40%) of the *ad libitum* intake of the unrestricted rats. Because the objective of this experiment was to study the effects of DER on energy sensing pathways in the liver, DER was maintained for 4 wk at which time the rats were euthanized.

**Necropsy and sample collection.** All rats were euthanized over a 3-h time interval each day. Following the routine overnight fast to which rats were accustomed, rats were euthanized via inhalation of gaseous carbon dioxide. The sequence in which rats were euthanized was stratified across groups to minimize the likelihood that order effects would masquerade as treatment associated effects. After the rats lost consciousness, the livers were immediately excised and frozen between clamps that were precooled in liquid nitrogen. The livers were put in plastic bags and the bags were sealed and then placed in liquid nitrogen. After transport from the animal facility, the frozen livers were stored at  $-80^{\circ}\text{C}$  until they were analyzed.

**Western blotting.** Mammary carcinomas, mammary gland, or liver was homogenized in lysis buffer [40 mmol/L Tris-HCl (pH 7.5), 1% Triton X-100, 0.25 mol/L sucrose, 3 mmol/L EGTA, 3 mmol/L EDTA, 50  $\mu\text{mol/L}$   $\beta$ -mercaptoethanol, 1 mmol/L phenyl-methylsulfonyl fluoride, and complete protease inhibitor cocktail (Calbiochem)]. The lysates were centrifuged at  $7,500 \times g$  for 10 min in a tabletop centrifuge at  $4^{\circ}\text{C}$  and clear supernatant fractions were collected and stored at  $-80^{\circ}\text{C}$ . The protein concentration in the supernatants was determined by the Bio-Rad protein assay.

Western blotting was done as described previously (6). Briefly, 40 to 60  $\mu\text{g}$  of protein lysate per sample were subjected to 8% to 16% SDS-PAGE after being denatured by boiling with SDS sample buffer [63 mmol/L Tris-HCl (pH 6.8), 2% SDS, 10% glycerol, 50 mmol/L DTT, and 0.01% bromophenol blue] for 5 min and the proteins were transferred onto a nitrocellulose membrane. The levels of LKB1, phospho-AMPK (Thr<sup>172</sup>), AMPK, phospho-mTOR (Ser<sup>2448</sup>), mTOR, phospho-p70S6K (Thr<sup>389</sup>), p70S6K, phospho-4E-BP1 (Thr<sup>37/46</sup>), 4E-BP1, phospho-ACC (Ser<sup>79</sup>), ACC, phospho-Akt (Ser<sup>473</sup>), Akt, IGF-IR, PI3Kp85, PI3Kp110 $\alpha$ , and  $\beta$ -actin were determined with specific primary antibodies, followed by treatment with the appropriate peroxidase-conjugated secondary antibodies, and visualized by LumiGLO reagent Western blotting detection system. The chemiluminescence signal was captured using a ChemiDoc densitometer (Bio-Rad) run under the control of Quantity One software (Bio-Rad). The actin-normalized scanning density data were reported.

**ELISA-based mTOR kinase activity assay.** For ELISA-based mTOR kinase activity assay (K-LISA, EMD), two steps were done as follows.

**Immunoprecipitation and kinase activity.** Clamp-frozen liver was homogenized in a specified lysis buffer [50 mmol/L Tris-HCl, 100 mmol/L NaCl, 50 mmol/L  $\beta$ -glycerophosphate, 10% glycerol (w/v), 1% Tween 20 detergent (w/v), 1 mmol/L EDTA, 20 nmol/L microcystin-LR, 25 mmol/L NaF, and a cocktail of protease inhibitors (EMD)]. Homogenates were centrifuged at  $16,000 \times g$  for 10 min at  $4^{\circ}\text{C}$  and the supernatant was

transferred to a clean tube. The supernatant (0.5 mL, protein concentration at 7 mg/mL) was precleared by adding 15  $\mu$ L of Protein G-Plus agarose beads, incubating for 15 min at 4°C, and centrifuged at 4,000  $\times$  *g* for 5 min at 4°C to pellet the agarose beads. Ten microliters of mTOR antibody (EMD) were added to the precleared lysates in fresh tubes and rotated for 1 h at 4°C. Then, 50  $\mu$ L of protein G-Plus agarose beads were added in the tube and rotated for 90 min at 4°C. The agarose beads were washed with lysis buffer thrice and with 1 $\times$  Kinase Assay Buffer (EMD) once and centrifuged at 4,000  $\times$  *g* for 5 min at 4°C. The beads were gently mixed with 2 $\times$  Kinase Assay Buffer working solution (2 $\times$  Kinase Assay Buffer, 20 mmol/L ATP, and 100 mmol/L DTT; EMD) and recombinant p70S6K-glutathione *S*-transferase fusion protein (EMD) to be evenly suspended, and incubated at 30°C for 30 min. The reaction was stopped by adding Stop Solution (EMD) and centrifuged at 4,000  $\times$  *g* for 5 min at 4°C and the supernatant was stored at -80°C until the assay can be completed.

**ELISA.** One hundred microliters of supernatant obtained from the kinase activity were added to each well of Glutathione-Coated 96-Well Plates (EMD) and incubated for 60 min at 30°C, followed by three washes with Plate Wash Buffer (EMD). Then, 100  $\mu$ L of anti-p70S6K-T389 Working Solution (EMD) were added to each well and incubated for 1 h at room temperature. After three washes with the Plate Wash Buffer, 100  $\mu$ L of HRP-antibody conjugate (EMD) were added to each well and incubated for 1 h at room temperature. After another three washes with the Plate Wash Buffer, 100  $\mu$ L of TMB substrate (EMD) were added and incubated for 20 min at room temperature, followed by the addition of 100- $\mu$ L ELISA Stop Solution (EMD) to each well. The plate was read at 450 to 595 nm. A serially diluted standard (enriched rat brain fraction, EMD), which was 50, 16.67, 5.56, 1.85, 0.62, and 0.21  $\mu$ L, was done at the same time. Because the activity unit of the mTOR standard was not provided by the company (EMD), the data were expressed as arbitrary units (i.e., microliter of standard). It has been suggested that the data can be expressed as the percent of the control.

#### Statistical analyses

Differences among groups in the incidence and multiplicity of mammary adenocarcinomas were evaluated, respectively, by  $\chi^2$  analysis (25) or ANOVA after square root transformation of tumor count, as recommended in ref. 26. Differences among groups in the body weight were analyzed by ANOVA and post hoc comparisons were done by method of Bonferroni (27). For Western blots, representative western bands were shown in the figures. The data displayed in the bar graphs of the figures were either the actin-normalized scanning data or the ratio of the actual scanning units derived from the densitometric analysis of each Western blot for the phospho-protein divided by its nonphosphorylated counterpart for proteins involved in energy sensing pathways. For statistical analyses, the actin-normalized scanning density data obtained with the ChemiDoc scanner (Bio-Rad) were

first rank transformed. This approach is particularly suitable for semiquantitative measurements that are collected as continuously distributed data, as is the case with Western blots. The ranked data were then subjected to ANOVA (experiment 1) or regression analysis (experiment 2; ref. 28). Ratio data were computed from the scanning units derived from the densitometric analysis (i.e., the arbitrary units of absorbance for variables stated and then the ratios were rank transformed and evaluated via ANOVA or regression analysis; ref. 28). All analyses done used Systat statistical analysis software, version 12.

## Results

### Experiment 1

#### Effects of DER on carcinogenic response and body weight.

Cancer incidence and multiplicity were reduced by DER in a dose-dependent manner as shown in Table 1. Cancer incidence was 96%, 60%, and 23% ( $P < 0.001$ ) and cancer multiplicity was 2.4, 1.1, and 0.3 carcinomas per rat ( $P < 0.001$ ) in control, 20% DER, and 40% DER treatment groups, respectively. DER resulted in lower final body weights that were 180, 150, and 123 g in the control, 20% DER, and 40% DER, respectively,  $P < 0.001$  (Table 1).

**Mammary carcinomas.** Because we have previously shown DER to dramatically decrease tumor mass by inhibiting cell proliferation and tumor vascularization and by promoting a proapoptotic environment (6, 8, 9, 29), the initial focus of our investigation was on mammary carcinomas.

**AMPK.** As shown in Fig. 1A, Western blot analysis on mammary carcinomas indicated that DER induced a 1.5-fold increase in the amount of LKB1, the kinase that phosphorylates AMPK on Thr<sup>172</sup> ( $P < 0.001$ ). Whereas DER caused a numerical decrease in the amount of AMPK present in mammary carcinomas ( $P = 0.32$ ), DER induced an increase in phosphorylated AMPK (Thr<sup>172</sup>;  $P < 0.001$ ); the amount of phosphorylated AMPK to AMPK was 1.6- and 2.8-fold higher at 20% and 40% DER versus control (0% DER), respectively. Parallel to the increase in AMPK activation, an increase in the ratio of phosphorylated ACC (Ser<sup>79</sup>)/ACC was observed in mammary carcinomas at both 20% DER (1.3-fold) and 40% DER (1.9-fold;  $P = 0.029$ ).

**mTOR, p70S6K, and 4E-BP1.** As shown in Fig. 1B, DER significantly decreased the ratio of phosphorylated mTOR (Ser<sup>2448</sup>)/mTOR ( $P < 0.001$ ), phosphorylated p70S6K (Thr<sup>389</sup>)/p70S6K ( $P < 0.05$ ), and phosphorylated 4E-BP1 (Thr<sup>37/46</sup>)/4E-BP1

**Table 1.** The overall effects of different levels of DER on body weight and mammary carcinogenesis

DER (%)	Experiment 1			Experiment 2	
	Final body weight (g)	Cancer incidence (%)	Cancer multiplicity (no./rat)	Final body weight (g)	Total body weight gain (g)
0	180 $\pm$ 3 <sup>a</sup>	96 <sup>a</sup>	2.4 $\pm$ 0.3 <sup>a</sup>	143 $\pm$ 3 <sup>a</sup>	95 $\pm$ 2 <sup>a</sup>
5	—	—	—	113 $\pm$ 1 <sup>b</sup>	68 $\pm$ 1 <sup>b</sup>
10	—	—	—	111 $\pm$ 1 <sup>b</sup>	66 $\pm$ 1 <sup>b</sup>
20	150 $\pm$ 1 <sup>b</sup>	60 <sup>b</sup>	1.1 $\pm$ 0.2 <sup>b</sup>	106 $\pm$ 1 <sup>bc</sup>	61 $\pm$ 1 <sup>b</sup>
40	123 $\pm$ 1 <sup>c</sup>	23 <sup>c</sup>	0.3 $\pm$ 0.083 <sup>c</sup>	94 $\pm$ 1 <sup>c</sup>	48 $\pm$ 1 <sup>c</sup>

NOTE: Experiment 1 was a mammary carcinogenesis study as described in Materials and Methods. The rats were fed either an unlimited amount of diet (DER 0%) or were restricted to 80% or 60% of *ad libitum* intake. In experiment 2, rats were not injected with carcinogen. Rats were fed either an unlimited amount of diet or were restricted to 95%, 90%, 80%, and 60% of the *ad libitum* intake (DER 5%, 10%, 20%, and 40%) as described in Materials and Methods. Values are means  $\pm$  SE for body weight and cancer multiplicity ( $n = 30$  in experiment 1,  $n = 8$  in experiment 2). Different superscripts (a-c) within the same column are statistically significant among the levels of energy intake ( $P < 0.05$ ).

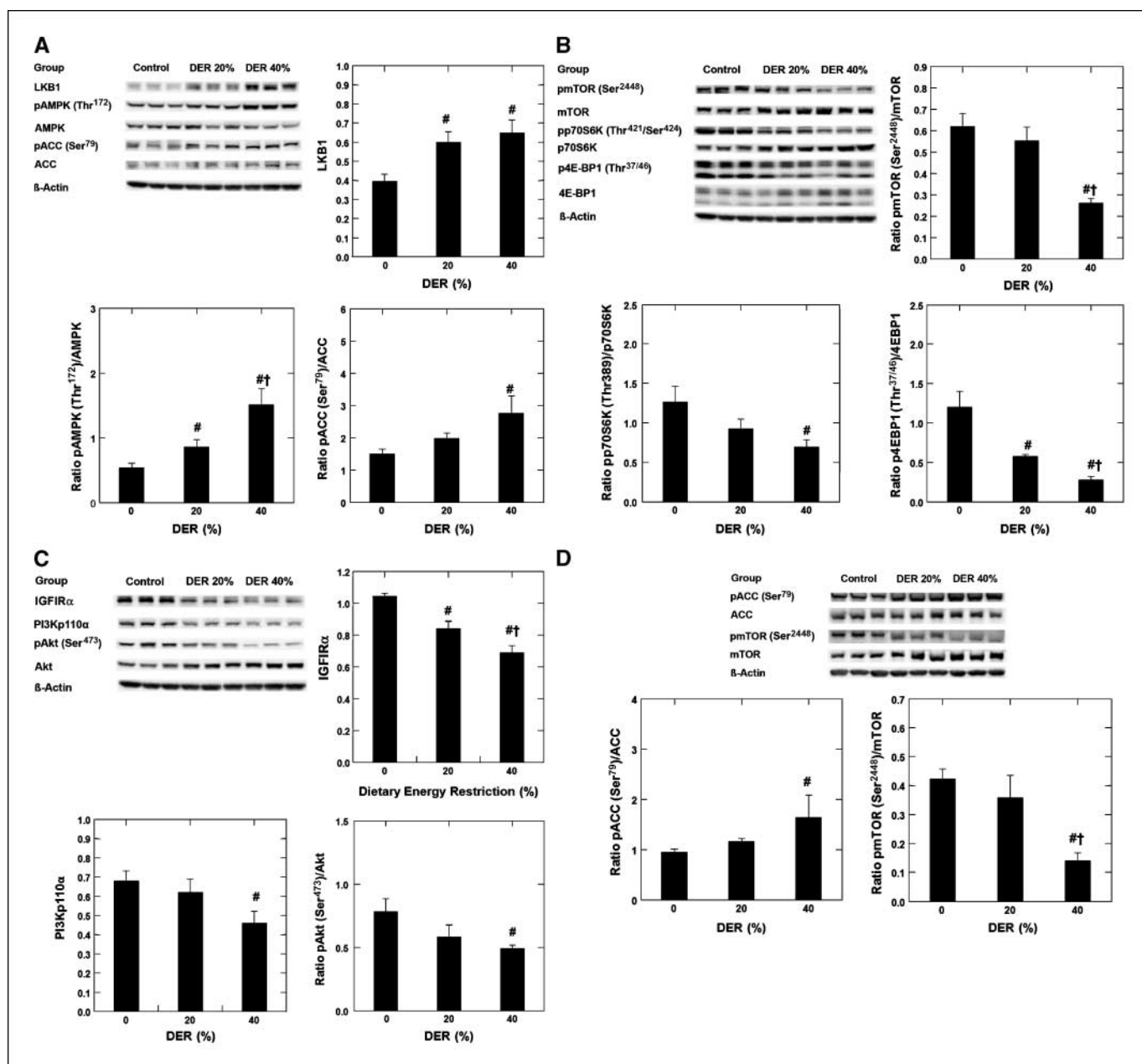


**Figure 1.** Effects of DER at 0% (control,  $n = 9$ ), 20% ( $n = 9$ ), or 40% ( $n = 7$ ) on LKB1; on the phosphorylation of AMPK (*pAMPK*; Thr<sup>172</sup>) and ACC (*pACC*; Ser<sup>79</sup>) in mammary carcinomas of rats (A); on the phosphorylation of mTOR (*pmTOR*; Ser<sup>2448</sup>), p70S6K (*pp70S6K*, Thr<sup>389</sup>), and 4E-BP1 (*p4E-BP1*, Thr<sup>37/46</sup>) in mammary carcinomas of rats (B); on the expression of IGF-IR $\alpha$ , PI3Kp110 $\alpha$ , and phosphorylated Akt (*pAkt*, Ser<sup>473</sup>) in mammary carcinomas of rats (C); and on the phosphorylation of ACC (Ser<sup>79</sup>) and mTOR (*pmTOR*, Ser<sup>2448</sup>) in mammary glands of rats (D). Representative Western blot images and bar graphs for the levels of proteins (normalized to  $\beta$ -actin) or the ratio of phosphorylated to unphosphorylated form are shown in each panel. The images shown are those directly acquired from the ChemiDoc work station which is equipped with a charge-coupled device camera having a resolution of  $1,300 \times 1,030$ . The normalized intensity data from the ChemiDoc were evaluated; statistical analyses were done on the ranks of the absorbance data via ANOVA and/or regression analysis. Bars, SE. #,  $P < 0.05$ , versus 0% DER; †,  $P < 0.05$ , versus 20% DER.

( $P < 0.001$ ). Compared with control (0% DER), the reduction was 11% or 58% for phosphorylated mTOR, 27% or 45% for phosphorylated p70S6K, and 52% or 77% for phosphorylated 4E-BP1 at 20% DER or 40% DER, respectively.

**IGF-IR, PI3K, and Akt.** As shown in Fig. 1C, DER was associated with a reduction in levels of IGF-IR $\alpha$  ( $P < 0.001$ ) and PI3Kp110 $\alpha$  ( $P = 0.033$ ) and the ratio of phosphorylated Akt (Ser<sup>473</sup>)/Akt ( $P = 0.033$ ). The reduction was 19% or 34% for IGF-IR $\alpha$ , 8% or 32%

for PI3Kp110 $\alpha$ , and 26% or 37% for phosphorylated Akt (Ser<sup>473</sup>) for 20% DER or 40% DER versus control (0% DER).

**Mammary gland.** AMPK activity was measured by the ratio of phosphorylated to total ACC. As shown in Fig. 1D, Western blot analysis indicated that the ratio of pACC (Ser<sup>79</sup>)/ACC was increased 1.2- or 1.7-fold by 20% DER or 40% DER ( $P = 0.034$ ). Moreover, the ratio of phosphorylated mTOR (Ser<sup>2448</sup>)/mTOR was reduced by 15% or 67% for 20% DER or 40% DER ( $P = 0.004$ ).

## Experiment 2

As described in Materials and Methods, a range of restricted energy intake was investigated that encompassed and expanded on those used in experiment 1. Western blot analyses were done on livers from all rats ( $n = 8$  per group) in this experiment so that we could robustly test our hypothesis about DER on AMPK, Akt, and mTOR using regression analysis. The overall effects of different levels of energy intake on body weight gain over the duration of this experiment are shown in Table 1. All rats were in positive energy balance (i.e., they gained weight).

### Liver

**AMPK.** Representative Western blots showing the effects of DER on the hepatic levels of AMPK and phosphorylated AMPK protein are shown in Fig. 2A. The amount of phosphorylated AMPK (Thr<sup>172</sup>) and their ratio increased ( $r = 0.82$ ,  $P < 0.001$ , and  $r = 0.93$ ,  $P < 0.001$ , respectively) with increasing DER.

**mTOR activity.** Hepatic mTOR activity was assessed directly with an ELISA-based assay as described in Materials and Methods. As shown in Fig. 2A, mTOR activity was inversely proportional to DER ( $r = -0.89$ ,  $P < 0.001$ ). The correlation between mTOR activity and phosphorylated mTOR (Ser<sup>2448</sup>) was also measured; the two measurements were highly correlated ( $r = 0.97$ ,  $P < 0.0001$ ; data not shown).

**p70S6K and 4E-BP1.** Levels of p70S6K and phosphorylated p70S6K protein both decreased with increasing DER ( $P < 0.01$ ; representative Western blots shown in Fig. 2B), and therefore we computed their ratio. As shown in Fig. 2B, there was a decrease in that ratio with increasing DER ( $r = -0.81$ ,  $P < 0.001$ ).

The effects of DER on the amounts of 4E-BP1 and phosphorylated 4E-BP1 (Thr<sup>37/46</sup>) are also shown in Fig. 2B. Levels of phosphorylated 4E-BP1 were marginally affected by DER ( $P = 0.001$ ), whereas there was a negative association ( $r = -0.65$ ,  $P = 0.001$ ) between DER and phosphorylated 4E-BP1 (Thr<sup>37/46</sup>). As shown in Fig. 2B, there was a decrease in the ratio of phosphorylated 4E-BP1 to 4E-BP1 with increasing DER ( $r = -0.66$ ,  $P < 0.001$ ).

**Akt.** A representative Western blot for Akt and phosphorylated Akt (Ser<sup>473</sup>) is shown in Fig. 2C. The level of Akt in the liver was not affected by DER ( $P = 0.51$ ), whereas there was a strong inverse association between the level of phosphorylated Akt (Ser<sup>473</sup>;  $r = -0.71$ ,  $P < 0.001$ ) and the ratio of phosphorylated Akt to Akt ( $r = -0.76$ ,  $P < 0.001$ ) with increasing DER. Based on the effects of DER on the levels of phosphorylated Akt, we predicted that there would be corresponding changes in levels of phosphorylated TSC2 at Thr<sup>1462</sup>, which is a substrate for phosphorylated Akt. Figure 2C shows representative Western blots for TSC2 and phosphorylated TSC2. Regression analysis of these Western data on DER indicated that the ratio of phosphorylated TSC2 to TSC2 decreased with increasing DER ( $r = -0.68$ ,  $P < 0.001$ ). A logical parallel to these analyses would have been the Western blot analysis of phosphorylated TSC2 (Ser<sup>1341/1337</sup>), the sites phosphorylated by AMPK; however, to date, none of the commercially available anti-phospho-protein antisera have been of sufficient specificity for use in Western blot analyses of rat tissue extracts.

## Discussion

Although a number of candidate mechanisms by which DER inhibits carcinogenesis have been proposed (3), the hypothesis that DER acts by modulating the activity of intracellular energy sensing pathways has previously not been tested. As shown in Fig. 1A, this

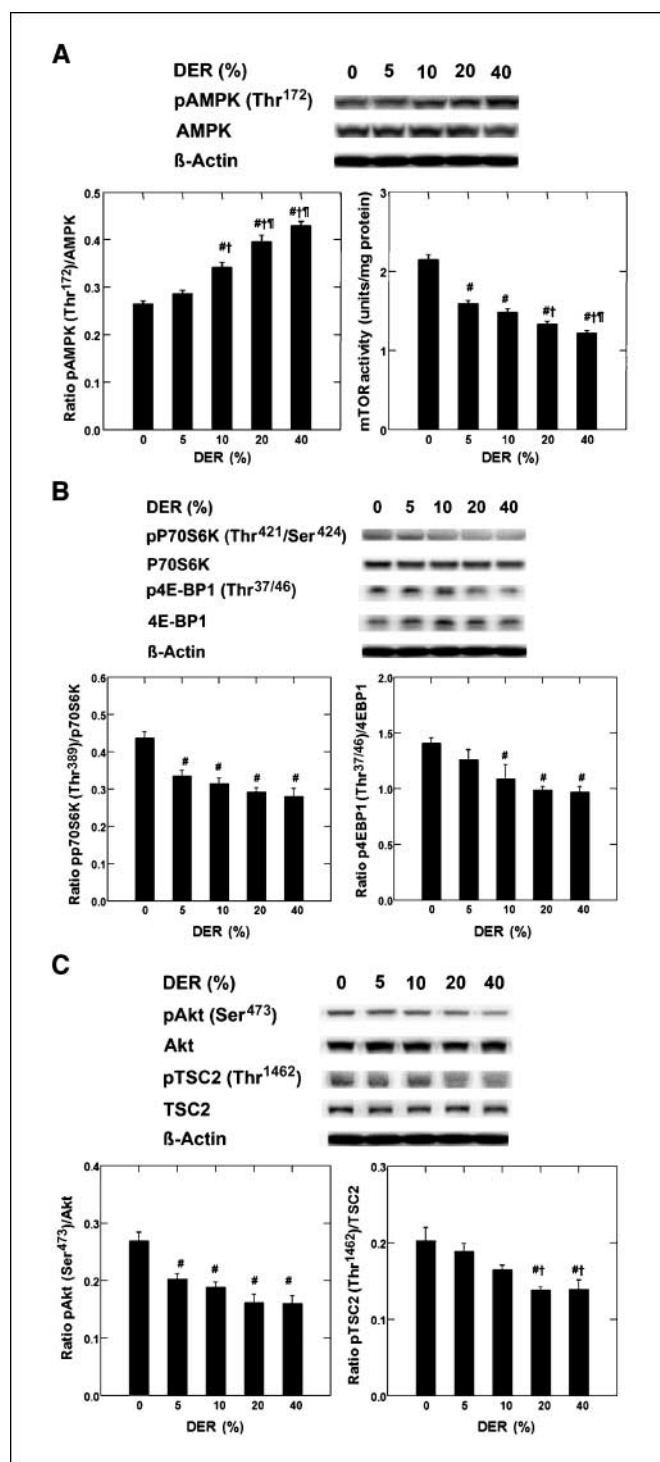


**Figure 2.** Effects of DER at 0%, 5%, 10%, 20%, or 40% on the phosphorylation of AMPK (Thr<sup>172</sup>) and the activity of mTOR in livers of rats (A), on the phosphorylation of p70S6K (pp70S6K, Thr<sup>389</sup>) and 4E-BP1 (p4E-BP1, Thr<sup>37/46</sup>; B), and on the phosphorylation of Akt (pAkt, Ser<sup>473</sup>) and TSC2 (pTSC2, Thr<sup>1462</sup>; C) in livers of rats ( $n = 8$ ). Representative Western blot images and bar graphs for the levels of proteins or activity or the ratio of phosphorylated to unphosphorylated form are shown in each panel. The images shown are those directly acquired from the ChemiDoc work station which is equipped with a charge-coupled device camera having a resolution of  $1,300 \times 1,030$ . The normalized intensity data from the ChemiDoc were evaluated; statistical analyses were done on the ranks of the absorbance data via regression analysis. The mTOR activity was determined by ELISA-based mTOR kinase activity assay and the data were analyzed by regression analysis. Bars, SE. #,  $P < 0.05$  versus 0% DER; †,  $P < 0.05$  versus 5% DER; ‡,  $P < 0.05$  versus 10% DER.

study reports the first evidence that DER induces the activation of a highly sensitive intracellular energy sensor (i.e., the phosphorylation of AMPK in mammary carcinomas) and that activation of AMPK in response to DER also occurs in mammary glands (Fig. 1D) and in the livers of non-carcinogen-treated rats (Fig. 2A). Furthermore, the effect of DER on this intracellular energy sensor seems to be coupled, in part, with its effects on the extracellular environment that are mediated via insulin-related growth factor signaling in a manner that affects the activity of mTOR. Key steps in the pathways affected by DER are diagrammed in Fig. 3 and are discussed in the following paragraphs.

**AMPK.** AMPK is an exquisitely sensitive detector of small changes in the cellular availability of ATP, and some investigators have even proposed that AMPK plays a central role in homeostatic regulation of whole-body energy metabolism (30). AMPK is activated via phosphorylation of Thr<sup>172</sup>, located on the  $\alpha$  catalytic subunit of this heterotrimeric protein. AMPK is phosphorylated on Thr<sup>172</sup> by constitutively active LKB1, a reaction that occurs due to conformational changes induced in the  $\gamma$  regulatory subunit of AMPK by its binding of AMP, an event that occurs with greater prevalence when the ratio of AMP/ATP increases within the cell (13). We studied the effects of DER on the levels of AMPK and phosphorylated AMPK (Thr<sup>172</sup>) and on LKB1. It was observed via Western blot analyses that the amount of phosphorylated AMPK and the ratio of phospho-AMPK/AMPK increased with increasing DER ( $P < 0.001$ ), indicative of strong activation response of AMPK to DER. To confirm that DER actually increased AMPK activity, the site-specific phosphorylation of ACC, a known substrate for AMPK, was measured. The

phosphorylation of ACC (Ser<sup>79</sup>) increased in response to DER. Given that ACC is not directly related to the energy sensing pathway that we were investigating, such independent confirmation of increased AMPK activity strengthens the observation that DER activates AMPK in mammary carcinomas. Moreover, given that inhibition of fatty acid synthesis has also been associated with anticancer activity, and that phosphorylation of Ser<sup>79</sup>-ACC by AMPK inhibits ACC activity, this observation suggests yet another mechanism by which DER may inhibit carcinogenesis (31, 32).

**LKB1.** LKB1 is generally reported to be constitutively active and is not usually considered a factor in determining whether AMPK responds to changes in intracellular energy availability signaled by the AMP/ATP ratio (33). However, Western blot analysis (Fig. 1A) indicated that the amount of LKB1 protein in mammary carcinomas was significantly increased in response to DER. The significance of this finding is unclear because the kinase activity of LKB1 was not measured, but available evidence does indicate that loss of LKB1 kinase activity underlies Peutz-Jeghers syndrome, and this has led to the observation that LKB1 is a tumor suppressor that exerts its effect, at least in part, via its kinase-mediated activation of AMPK (reviewed in ref. 32). Hence, the possibility that DER induces the tumor suppressor activity of the protein complex in which LKB1 participates (STE-related adaptor, mouse protein 25, LKB1) merits further investigation.

We extended our investigation of DER and AMPK to mammary gland but focused on AMPK activity as indicated by phospho-ACC (Ser<sup>79</sup>) because of the limited amount of mammary gland that was available from experiment 1. As shown in Fig. 1D, the amount of phospho-ACC and the ratio pACC/ACC increased with DER, suggesting that the effect of DER extends to cells that are not directly involved in carcinogenesis. We further tested this idea by assessing the activation of AMPK in livers of non-carcinogen-treated rats with the benefit of the relative homogeneity of cell types within liver versus either mammary carcinoma or mammary gland. A highly significant positive relationship was observed between activated AMPK and magnitude of DER (Fig. 2A); in fact, DER accounted for 61% of the variation in activated AMPK. Collectively, these observations were consistent with emerging evidence that AMPK functions as a cellular energy sensor (34) and that DER activates AMPK in both cancer cells and in cells of tissues not involved in the carcinogenic process. AMPK activity was highest when energy intake was lowest and activity was down-regulated as energy intake increased.

**mTOR.** Activated AMPK has a number of targets that are likely to be directly relevant to carcinogenesis (32), but in this study, we focused on mTOR, an evolutionarily conserved serine-threonine kinase that is a key regulator of protein translation and synthesis. This kinase is centrally involved in cell growth (i.e., increase in cell size and cell mass, and these processes are tightly coupled to cell division; reviewed in ref. 32). The mTOR pathway integrates nutrient, energy, and mitogen signals to regulate cell growth and cell division (35–37). Activated AMPK has been reported to suppress mTOR activity through the maintenance of the GTPase activity of RHEB protein via site-specific phosphorylation of TSC2 at Ser<sup>1337</sup> and Ser<sup>1341</sup>. As shown in Fig. 1B, DER reduced levels of phospho-mTOR, which we showed to be highly correlated with mTOR activity in liver. We next determined the effect of DER on phospho-mTOR in the mammary gland, and as shown in Fig. 1D, DER significantly reduced its phosphorylation. As shown in Fig. 2A, the down-regulation of mTOR activity in liver was shown by a direct assessment of its activity.

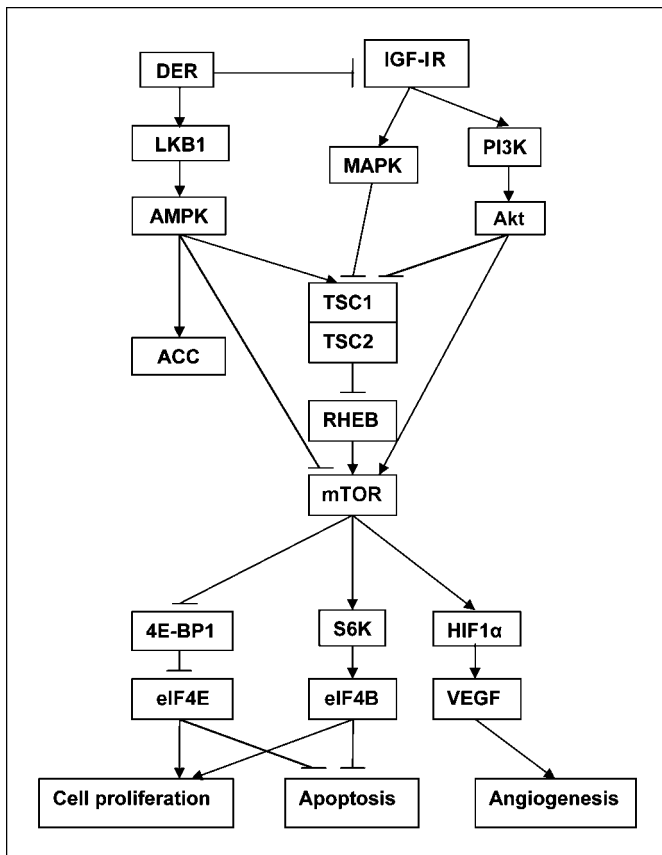


Figure 3. Energy sensing pathways affected by DER.

**p70S6 kinase and 4E-BP1.** Because mTOR affects a complex array of signaling events, we decided to further investigate the effects of DER on the phosphorylation of two proteins, p70S6K and 4E-BP1, which are substrates of mTOR (38–40). Activated mTOR phosphorylates p70S6K, and this leads to increased ribosomal biogenesis (41, 42). 4E-BP1 is a repressor of translation initiation (40, 43). Activated mTOR phosphorylates 4E-BP1, which inactivates the protein. When it is hypophosphorylated, 4E-BP1 binds to and inhibits the rate-limiting translation initiation factor eIF4E (eukaryotic translation initiation factor 4E). On phosphorylation, eIF4E is released from 4E-BP1, allowing eIF4E to assemble with other translation initiation factors to initiate cap-dependent translation (44). These analyses were only done in mammary carcinomas and liver. As shown in Figs. 1B and 2B, phosphorylation of p70S6 kinase and 4E-BP1 was significantly reduced in mammary carcinomas and liver by DER. These findings are consistent with the down-regulation of mTOR activity by DER and indicate that DER is likely to inhibit cell growth and cell division via mTOR-mediated effects on protein synthesis. Relative to a chronic disease process such as carcinogenesis, this suggests that the propensity for altered patterns of gene expression that occur during clonal selection and expansion of transformed cell populations would be suppressed by DER, a finding consistent with our previous observations (23, 29, 45).

**Akt.** DER has been reported by us to decrease the circulating levels of IGF-I (10), and reduced levels of circulating IGF-I would be expected to down-regulate signaling via the pathway whose components are IGF-IR, PI3K, and Akt. Of these proteins, activated Akt, a serine/threonine kinase, is the critical effector molecule. Phospho-Akt serves important roles in cell proliferation, cell survival, and new blood vessel formation that are associated with tumor development (3). Therefore, our investigation was extended to these molecules because emerging evidence indicates that the effects of this pathway are also, in part, mediated via mTOR (17–20). The linkage of this pathway to mTOR is specifically attributed to phosphorylated Akt, which has been reported to oppose the effects of phosphorylated AMPK on the activity of mTOR and its upstream targets via phosphorylation of Ser<sup>1345</sup> and Thr<sup>1227</sup> on TSC2 (21). As shown in Figs. 1C and 2C, effects on activated Akt were marked and DER was observed to reduce levels of phospho-Akt (total amount or the ratio of phospho-Akt/Akt) in both mammary carcinomas and liver. Whereas it is clear that reduced levels of activated Akt are likely to affect proliferation, apoptosis, and angiogenesis by mechanisms independent of mTOR (reviewed in ref. 46), the finding that DER induces dual events, AMPK activation and down-regulation of growth factor signaling

via Akt, which are integrated via TSC2 to decrease mTOR activity, is a currently unappreciated dimension in elucidating the mechanisms that account for the profound ability of DER to inhibit the carcinogenic process.

**Summary and implications.** These findings provide important insights about the DER mechanisms of action and are likely to have significant translational implications. Whereas evidence continues to grow, indicating that limiting energy availability to an organism has beneficial effects against a number of chronic diseases and also prolongs survival (i.e., retards aging), most efforts to identify common causal links have focused on signaling via insulin and IGFs and processes such as reduced cellular oxidation. Our finding that DER induces the activation of AMPK provides a new lens through which to search for common causal mechanisms that account for the health benefits of DER. For many years, the control of type 2 diabetes and hyperlipidemia syndromes has been a goal of drug development efforts that directly or indirectly target the activation of AMPK. One of the most widely used of the drugs thus far developed is metformin (47), and emerging evidence is suggestive of reduced cancer rates in individuals who have taken metformin for the control of type 2 diabetes (48). We have also recently reported that 2-deoxy-glucose induces the activation of AMPK *in vivo*, and we suspect that this accounts, at least part, for its ability to inhibit experimentally induced breast cancer (49). Moreover, to the extent that activation of AMPK and down-regulation of Akt by DER mediate their effects on carcinogenesis via mTOR, the area of DER now intersects with three signaling pathways of current interest as new targets for development of cancer therapeutics. Those efforts may now be seen as opportunities to co-develop energy restriction mimetic agents as defined in ref. 49. In summary, this work identifies components of intracellular energy sensing pathways, specifically mTOR, its principal upstream regulators, AMPK and Akt, and its downstream targets, p70S6K and 4E-BP1, as candidate molecules on which to center mechanistic studies of DER.

## Disclosure of Potential Conflicts of Interest

No potential conflicts of interest were disclosed.

## Acknowledgments

Received 12/20/2007; revised 3/28/2008; accepted 4/28/2008.

**Grant support:** USPHS grant CA52626 from the National Cancer Institute.

The costs of publication of this article were defrayed in part by the payment of page charges. This article must therefore be hereby marked *advertisement* in accordance with 18 U.S.C. Section 1734 solely to indicate this fact.

## References

- Birt DF, Kris ES, Choe M, Pelling JC. Dietary energy and fat effects on tumor promotion. *Cancer Res* 1992;52:2035–9s.
- Fu PP, Dooley KL, Von Tungeln LS, Bucci T, Hart RW, Kadlubar FF. Caloric restriction profoundly inhibits liver tumor formation after initiation by 6-nitrochrysene in male mice. *Carcinogenesis* 1994;15:159–61.
- Hursting SD, Lavigne JA, Berrigan D, Perkins SN, Barrett JC. Calorie restriction, aging, and cancer prevention: mechanisms of action and applicability to humans. *Annu Rev Med* 2003;54:131–52.
- Thompson HJ, Zhu Z, Jiang W. Dietary energy restriction in breast cancer prevention. *J Mammary Gland Biol Neoplasia* 2003;8:133–42.
- Yoshida K, Inoue T, Hirabayashi Y, Nojima K, Sado T. Calorie restriction and spontaneous hepatic tumors in C3H/He mice. *J Nutr Health Aging* 1999;3:121–6.
- Jiang W, Zhu Z, Thompson HJ. Effect of energy restriction on cell cycle machinery in 1-methyl-1-nitrosourea-induced mammary carcinomas in rats. *Cancer Res* 2003;63:1228–34.
- Jiang W, Zhu Z, McGinley JN, Thompson HJ. Adrenalectomy does not block the inhibition of mammary carcinogenesis by dietary energy restriction in rats. *J Nutr* 2004;134:1152–6.
- Thompson HJ, Zhu Z, Jiang W. Identification of the apoptosis activation cascade induced in mammary carcinomas by energy restriction. *Cancer Res* 2004;64:1541–5.
- Thompson HJ, McGinley JN, Spoelstra NS, Jiang W, Zhu Z, Wolfe P. Effect of dietary energy restriction on vascular density during mammary carcinogenesis. *Cancer Res* 2004;64:5643–50.
- Zhu Z, Jiang W, McGinley J, Wolfe P, Thompson HJ. Effects of dietary energy repletion and IGF-1 infusion on the inhibition of mammary carcinogenesis by dietary energy restriction. *Mol Carcinog* 2005;42:170–6.
- Pan JG, Mak TW. Metabolic targeting as an anticancer strategy: dawn of a new era? *Sci STKE* 2007;2007:pe14.
- Shaw RJ. Glucose metabolism and cancer. *Curr Opin Cell Biol* 2006;18:598–608.
- Hardie DG, Carling D. The AMP-activated protein kinase—fuel gauge of the mammalian cell? *Eur J Biochem* 1997;246:259–73.
- Bolster DR, Crozier SJ, Kimball SR, Jefferson LS.

- AMP-activated protein kinase suppresses protein synthesis in rat skeletal muscle through down-regulated mammalian target of rapamycin (mTOR) signaling. *J Biol Chem* 2002;277:23977–80.
15. Kimura N, Tokunaga C, Dalal S, et al. A possible linkage between AMP-activated protein kinase (AMPK) and mammalian target of rapamycin (mTOR) signalling pathway. *Genes Cells* 2003;8:65–79.
  16. Krause U, Bertrand L, Hue L. Control of p70 ribosomal protein S6 kinase and acetyl-CoA carboxylase by AMP-activated protein kinase and protein phosphatases in isolated hepatocytes. *Eur J Biochem* 2002;269:3751–9.
  17. Fang Y, Vilella-Bach M, Bachmann R, Flanigan A, Chen J. Phosphatidic acid-mediated mitogenic activation of mTOR signaling. *Science* 2001;294:1942–5.
  18. Gerasimovskaya EV, Tucker DA, Weiser-Evans M, et al. Extracellular ATP-induced proliferation of adventitial fibroblasts requires phosphoinositide 3-kinase, Akt, mammalian target of rapamycin, and p70 S6 kinase signaling pathways. *J Biol Chem* 2005;280:1838–48.
  19. Nave BT, Ouwens M, Withers DJ, Alessi DR, Shepherd PR. Mammalian target of rapamycin is a direct target for protein kinase B: identification of a convergence point for opposing effects of insulin and amino-acid deficiency on protein translation. *Biochem J* 1999;344:427–31.
  20. Peterson RT, Beal PA, Comb MJ, Schreiber SL. FKBP12-rapamycin-associated protein (FRAP) autophosphorylates at serine 2481 under translationally repressive conditions. *J Biol Chem* 2000;275:7416–23.
  21. Kwiatkowski DJ, Manning BD. Tuberous sclerosis: a GAP at the crossroads of multiple signaling pathways. *Hum Mol Genet* 2005;14:R251–258.
  22. James SJ, Muskhelishvili L. Rates of apoptosis and proliferation vary with caloric intake and may influence incidence of spontaneous hepatoma in C57BL/6 x C3H F1 mice. *Cancer Res* 1994;54:5508–10.
  23. Zhu Z, Haegele AD, Thompson HJ. Effect of caloric restriction on pre-malignant and malignant stages of mammary carcinogenesis. *Carcinogenesis* 1997;18:1007–12.
  24. Thompson HJ. Methods for the induction of mammary carcinogenesis in the rat using either 7,12-dimethylbenz(a)anthracene or 1-methyl-1-nitrosourea. In: Ip MM, Asch BB, editors. *Methods in mammary gland biology and breast cancer research*. New York: Kluwer Academic/Plenum Publishers; 2000. p. 19–29.
  25. Snedecor GW, Cochran WG. *Statistical methods*. 8th ed. Ames (IA): Iowa State University Press; 1989.
  26. Sokal RR, Rohlf FJ. *Biometry the principles and practice of statistics in biological research*. 3rd ed. New York: W.H. Freeman; 1995.
  27. Hochberg Y, Tamhane AC. *Multiple comparison procedures*. New York (NY): John Wiley & Sons, Inc.; 1987.
  28. Morrison DF. *Multivariate statistical methods*. 3rd ed. New York: McGraw-Hill Publishing Co.; 1990.
  29. Zhu Z, Jiang W, Thompson HJ. Effect of energy restriction on tissue size regulation during chemically induced mammary carcinogenesis. *Carcinogenesis* 1999;20:1721–6.
  30. Hardie DG. The AMP-activated protein kinase pathway—new players upstream and downstream. *J Cell Sci* 2004;117:5479–87.
  31. Brunet J, Vazquez-Martin A, Colomer R, Grana-Suarez B, Martin-Castillo B, Menendez JA. BRCA1 and acetyl-CoA carboxylase: the metabolic syndrome of breast cancer. *Mol Carcinog* 2008;47:157–63.
  32. Motoshima H, Goldstein BJ, Igata M, Araki E. AMPK and cell proliferation-AMPK as a therapeutic target for atherosclerosis and cancer. *J Physiol* 2006;574:63–71.
  33. Hardie DG. New roles for the LKB1→AMPK pathway. *Curr Opin Cell Biol* 2005;17:167–73.
  34. Hardie DG, Hawley SA, Scott JW. AMP-activated protein kinase—development of the energy sensor concept. *J Physiol* 2006;574:7–15.
  35. Hay N, Sonenberg N. Upstream and downstream of mTOR. *Genes Dev* 2004;18:1926–45.
  36. Kahn BB, Alquier T, Carling D, Hardie DG. AMP-activated protein kinase: ancient energy gauge provides clues to modern understanding of metabolism. *Cell Metab* 2005;1:15–25.
  37. Wullschlegler S, Loewith R, Hall MN. TOR signaling in growth and metabolism. *Cell* 2006;124:471–84.
  38. Gingras AC, Kennedy SG, O’Leary MA, Sonenberg N, Hay N. 4E-BP1, a repressor of mRNA translation, is phosphorylated and inactivated by the Akt(PKB) signaling pathway. *Genes Dev* 1998;12:502–13.
  39. Inoki K, Zhu T, Guan KL. TSC2 mediates cellular energy response to control cell growth and survival. *Cell* 2003;115:577–90.
  40. Martin KA, Blenis J. Coordinate regulation of translation by the PI 3-kinase and mTOR pathways. *Adv Cancer Res* 2002;86:1–39.
  41. Lee CC, Huang CC, Wu MY, Hsu KS. Insulin stimulates postsynaptic density-95 protein translation via the phosphoinositide 3-kinase-Akt-mammalian target of rapamycin signaling pathway. *J Biol Chem* 2005;280:18543–50.
  42. Martin KA, Rzcudlo EM, Merenick BL, et al. The mTOR/p70 S6K1 pathway regulates vascular smooth muscle cell differentiation. *Am J Physiol Cell Physiol* 2004;286:C507–517.
  43. Gingras AC, Raught B, Sonenberg N. Regulation of translation initiation by FRAP/mTOR. *Genes Dev* 2001;15:807–26.
  44. Sonenberg N, Gingras AC. The mRNA 5’ cap-binding protein eIF4E and control of cell growth. *Curr Opin Cell Biol* 1998;10:268–75.
  45. Zhu Z, Jiang W, Thompson HJ. Effect of energy restriction on the expression of cyclin D1 and p27 during premalignant and malignant stages of chemically induced mammary carcinogenesis. *Mol Carcinog* 1999;24:241–5.
  46. Younes H, Leleu X, Hatjiharissi E, et al. Targeting the phosphatidylinositol 3-kinase pathway in multiple myeloma. *Clin Cancer Res* 2007;13:3771–5.
  47. Hardie DG. AMP-activated protein kinase as a drug target. *Annu Rev Pharmacol Toxicol* 2007;47:185–210.
  48. Evans JM, Donnelly LA, Emslie-Smith AM, Alessi DR, Morris AD. Metformin and reduced risk of cancer in diabetic patients. *BMJ* 2005;330:1304–5.
  49. Zhu Z, Jiang W, McGinley JN, Thompson HJ. 2-Deoxyglucose as an energy restriction mimetic agent: effects on mammary carcinogenesis and on mammary tumor cell growth *in vitro*. *Cancer Res* 2005;65:7023–30.